

Estimation of Equivalent Current Distribution of Modulated EM Radiation Source

Bunka Nishina and Qiang Chen, *Senior Member, IEEE*

Abstract—To take effective measures for the interference problem between electronic devices, it is important to estimate the equivalent current distribution that is equivalent to the radiation source of unnecessary electromagnetic waves inside the electronic devices. Information of the equivalent current distribution could provide us some important knowledge to analyze the radiation source which could be the source of the EM interference. Previously, most of the researches have focused on estimating the location of CW electromagnetic radiation source in frequency domain. In this paper, a method including near field measurement in time domain and matrix inversion is proposed to estimate the equivalent current distribution of incoherent radiation source. The validity of this method is demonstrated using numerical simulations and experiments.

Index Terms—Antenna measurements, eigenvalues and eigenfunctions, electromagnetic compatibility, electromagnetic interference, equivalent sources, matrix inversion, near-field far-field transformation, time domain measurements.

I. INTRODUCTION

RECENTLY, the electromagnetic interference problem has become more and more serious because of miniaturization of the electrical devices and increase in operation frequency. To take effective measures for the interference problem, it is required to estimate the equivalent current distribution of the radiation source in the electric devices which radiate unnecessary electromagnetic waves. Information of the equivalent current distribution could provide us some important knowledge to analyze the radiation source which could be the source of the EM interference. From the earlier studies, the microwave imaging method where the radiation source is replaced with a set of equivalent sources is well known. This method was originally used to calculate the radiation from aperture antennas, which are replaced by the equivalent magnetic current located at equally spaced meshes of a two-dimensional plane [1], [2]. The advantage of this method is that the distribution of the equivalent radiation source can be estimated even if the position and the structure of the real source are unknown. The information of distribution of the equivalent radiation source could be helpful in diagnosing how the unnecessary electromagnetic wave is radiated from the electric device [3], [4]. Because the current distribution on the equivalent source is finally obtained by inverting the matrix of mutual impedance between the probe

and the equivalent source, the microwave imaging method has been applied to the problems in frequency domain and is valid for the coherent radiation source such as CW electromagnetic radiation source, but is invalid for incoherent radiation source such as modulated radiation source. When measuring the coherent radiation, the phase of field distribution can be obtained. However, when the radiation is random or incoherent, phase reference cannot be defined, making a measurement method in frequency domain impractical. In practice, the interference between electronic devices is usually caused by incoherent electromagnetic field and broadband signals. Therefore, it is very necessary to study and improve this measurement method to characterize the incoherent radiation sources.

In this research, an approach is proposed to construct the equivalent source for incoherent radiation. The time-domain near-field (TDNF) method [5], [6] is applied to measure the near field from the modulated radiation in time domain, and then a matrix equation is established in frequency domain from the correlation analysis of the measured near field distribution. Finally, the current distribution of equivalent radiation source is estimated by solving the matrix equation. The basic idea was introduced in the conference paper [7]; this paper has been largely enhanced by adding the details of the method and results of numerical simulations and measurements.

This paper is organized as follows. In Section II, the proposed method is introduced. The numerical simulation using the proposed method for two types of sources composed of dipole antennas is shown in Section III. In Section IV, estimation of the equivalent current distribution is performed experimentally for two types of sources: dipole antennas and microwave oven. Finally, conclusion is given in Section V.

II. MEASUREMENT METHOD

The proposed method is composed of two steps. First, the near field of a radiation source, which is fed with modulated signals at a center frequency f , is measured in time domain using the TDNF method. Subsequently, matrix inversion is applied to the construction of equivalent current distribution on the equivalent source using the eigenvalues and eigenvectors obtained from the near field measurement.

Let us consider that the incoherent source is enclosed by a measurement spherical surface Σ as shown in Fig. 1. The near field of the source is measured in time domain on the surface. Since the modulated radiation source radiates time-varying field, the field measured at different locations is incoherent and the phase reference is irrelevant. Therefore, the phase reference must be taken simultaneously at different locations on the

Manuscript received December 22, 2014; revised December 03, 2015; accepted December 29, 2015. Date of publication February 05, 2016; date of current version April 05, 2016.

The authors are with Tohoku University, Sendai 980-8579, Japan (e-mail: chenq@ecei.tohoku.ac.jp).

Color versions of one or more of the figures in this paper are available online at <http://ieeexplore.ieee.org>.

Digital Object Identifier 10.1109/TAP.2016.2526080

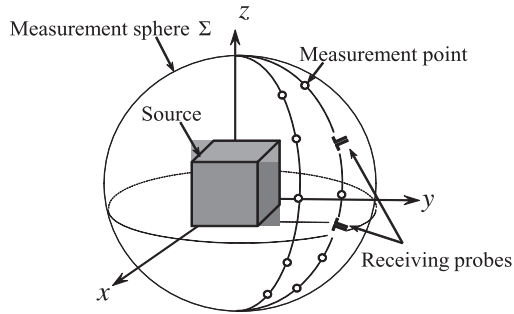


Fig. 1. Geometry of near field measurement.

measurement surface. For this reason, two probes are used to measure the near field simultaneously on the measurement surface. As shown in Fig. 1, the near field $E^\theta(t)$ and $E^\phi(t)$ are measured at the N -point positions on the surface enclosing the radiation source. The correlation between the measured field for every pair of measurement points is calculated to form a $2N \times 2N$ coherence matrix \mathbf{C} as follows:

$$\mathbf{C}_{2N \times 2N} = \begin{bmatrix} \mathbf{C}^{\theta\theta} & \mathbf{C}^{\theta\phi} \\ \mathbf{C}^{\phi\theta} & \mathbf{C}^{\phi\phi} \end{bmatrix} \quad (1)$$

where, e.g., $\mathbf{C}^{\theta\phi}$ indicates the coherence matrix element of the ϕ -polarized component with respect to θ -polarized component and its element is the correlation between the electric field measured at points i and j as follows:

$$C_{i,j}^{\theta\phi} = \frac{1}{T} \int_{t=0}^T E_i^\theta(t) E_j^{\phi*}(t) dt \quad (i, j = 1, 2, \dots, N) \quad (2)$$

where T is the total measurement time at one measurement point, and the superscript $*$ denotes the complex conjugate. T should be long enough to catch the modulated signal including the lowest frequency component to be concerned. Eigenvalue decomposition is performed for the correlation matrix \mathbf{C}

$$\mathbf{C} = \Phi_\Sigma \mathbf{\Lambda} \Phi_\Sigma^H + \sigma^2 \mathbf{I} \quad (3)$$

where σ^2 is the spectral density of noise, \mathbf{I} is the identity matrix, $\Phi_\Sigma = [\phi_1, \dots, \phi_{2N}]$ is the matrix composed of the eigenvectors ϕ_i which represent the eigenfunctions of the fields sampled at the N points on the surface Σ for both θ and ϕ components, and $\mathbf{\Lambda}$ is the diagonal matrix of eigenvalues $\text{diag}(\mathbf{\Lambda}) = [\lambda_1, \lambda_2, \dots, \lambda_{2N}]$. The eigenvalues are ordered as

$$\lambda_1 > \lambda_2 > \dots > \lambda_P > \sigma^2 > \lambda_{P+1} > \dots > \lambda_{2N}. \quad (4)$$

The top P eigenvalues are saved whereas the others corresponding to noise are discarded [8]. Therefore, P eigenvalues ($\lambda_1 \sim \lambda_P$) and corresponding eigenvectors ($\phi_1 \sim \phi_P$) are picked out to generate equivalent eigenmodes ($\lambda_1 \phi_1 \sim \lambda_P \phi_P$) which are considered to be coherent and orthogonal to each other. According to Mercer's theorem [9], [10], \mathbf{C} can be written as

$$\mathbf{C} = \sum_n \lambda_n \phi_n, \quad n = 1, 2, \dots, P \quad (5)$$

where ϕ_n are the eigenfunctions of \mathbf{C} on measurement sphere Σ , and λ_n are the eigenvalues which indicate the mean power

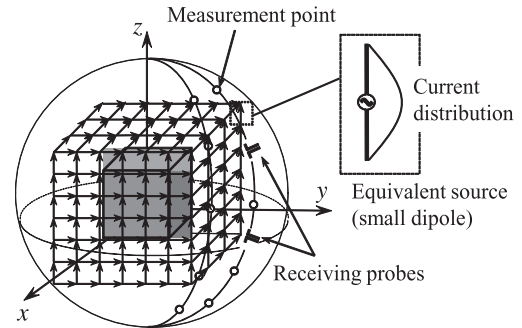


Fig. 2. Model of the equivalent source.

averaged over time of the n th source. Because eigenfunctions or correlation eigenvectors are orthogonal to each other, (5) provides a physical meaning that the incoherent field distribution can be decomposed into multiple coherent-like field distribution on the spherical surface Σ and the field distribution of each coherent-like field distribution is orthogonal to each other. Thus, the total field is written as the summation of multiple equivalent eigenmodes ($\lambda_1 \phi_1 \sim \lambda_P \phi_P$).

A model of equivalent source is established inside the spherical surface as shown in Fig. 2. The equivalent source is composed of electrically small dipoles with three polarizations and the dipoles are located at equally spaced meshes in an estimation area covering the real radiation source. The total number of the small dipoles is M . The current distribution on the real source is expressed in terms of the expansion function as follows:

$$\mathbf{I}(\mathbf{r}) = \sum_{j=1}^M I_j \mathbf{f}_j(\mathbf{r}) \quad (6)$$

where I_j is the unknown current coefficient on the j th dipole and the expansion function $\mathbf{f}_j(\mathbf{r})$ is a sinusoidal function indicating the current distribution on the j th dipole. The electrical field radiated by equivalent source $\mathbf{I}(\mathbf{r})$ becomes

$$\mathbf{E}(\mathbf{r}) = \int \overline{\mathbf{G}}(\mathbf{r}, \mathbf{r}') \cdot \mathbf{I}(\mathbf{r}') d\mathbf{r}' \quad (7)$$

where $\overline{\mathbf{G}}(\mathbf{r}, \mathbf{r}')$ is the dyadic Green's function in free space. Equation $\mathbf{E} = \mathbf{G}\mathbf{I}$ can be expressed into the following linear matrix equation using the concept of reaction integrals in the method of moments [11]

$$V_i = \sum_{j=1}^M Z_{ij} I_j, \quad i = 1, 2, \dots, 2N \quad (8)$$

where V_i is the receiving voltage at position i on the measurement surface, and the impedance matrix Z_{ij} is the mutual impedance between the j th dipole of the equivalent source and the receiving probe at position i . The impedance matrix can be calculated as

$$Z_{ij} = \frac{1}{I_j} \int \mathbf{E}(\mathbf{r}) \cdot \mathbf{w}_i(\mathbf{r}) d\mathbf{r} \quad (9)$$

where $\mathbf{w}_i(\mathbf{r})$ is a sinusoidal function expressing the current distribution on the wire dipole for receiving, and the integration is applied along the probe which is electrically small. In

this paper, both function f in (6) and function w in (9) were sinusoidal function, and Z_{ij} defined in (9) becomes the mutual impedance between the electrically small dipoles in the equivalent source and the electrically small probe of electric field. Calculation of (9) is described in some references [12], [13].

V_i in (8) is the receiving voltage by the probe, and it is a complex value including magnitude and phase information. In this research, we propose to apply the eigenmodes $\lambda_p \phi_p$ ($p = 1 \sim P$) measured in the previous steps as the receiving voltage vector $\mathbf{V}^p = [\lambda_1 \phi_1, \dots, \lambda_P \phi_P]$. The multiple eigenmodes $\lambda_p \phi_p$ ($p = 1 \sim P$) which are orthogonal to each other can be obtained from the near field of the source. As each eigenmode is coherent, the total current distribution can be estimated by summing up the equivalent current distribution corresponding to each eigenmode.

Consequently, the unknown equivalent current distribution of radiation source is obtained by solving the matrix equation

$$\mathbf{V} = \mathbf{Z} \mathbf{I} \quad (10)$$

$2N \times P \quad 2N \times M \quad M \times P$

where \mathbf{V} vector is radiation field distribution of the radiation source composed of the equivalent eigenmodes $\lambda_p \phi_p$, and \mathbf{Z} matrix is the mutual impedance between the equivalent source and the two measurement probes. The unknown matrix \mathbf{I} is composed of M current coefficients on small dipoles of the equivalent source for P eigenmodes. Since the number of measurement points N is usually larger than that of equivalent source M , (10) can be solved by generalized matrix inversion, and the matrix \mathbf{I} of current coefficients on the equivalent source are obtained by solving

$$[\mathbf{I}^p] = [\mathbf{Z}^H \mathbf{Z}]^{-1} [\mathbf{Z}^H \mathbf{V}^p] \quad (N \geq M). \quad (11)$$

As each eigenmode $\lambda_p \phi_p$ ($p = 1 \sim P$) is orthogonal to each other, each current coefficient on the equivalent source can also be considered as coherent. Therefore, it is possible to estimate the total equivalent current distribution of the radiation source by adding together the components of $[\mathbf{I}]$ as

$$|\mathbf{I}| = \sqrt{|\mathbf{I}_1|^2 + \dots + |\mathbf{I}_P|^2}. \quad (12)$$

III. NUMERICAL SIMULATIONS

Two half-wavelength dipole antennas with y -polarization are placed in the estimation area as shown in Fig. 3. These two antennas are fed with continuous wave but the frequency is a little bit different, forming a modulated radiation source. Current on these dipoles can be expressed as $I_1 = I_0 e^{j\omega_c t}$ and $I_2 = I_0 e^{j(\omega_c + \Delta\omega)t}$. Some parameters of the source model for numerical simulation are shown in detail in Table I.

The simulation model including the source model and measurement plane is illustrated in Fig. 4. The measurement plane is aligned on the x - y plane and located at $z = 0$. The total measurement points are N . The distance between the measurement plane and estimation plane is r . Interval of the measurement points is 0.08λ . The x , y -polarized electric fields are measured at each measurement point.

The estimation area is a $2\lambda \times 2\lambda$ square plane that is parallel to the measurement plane as shown in Fig. 5. The equivalent

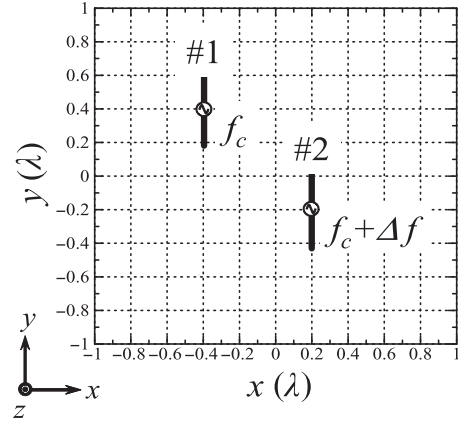


Fig. 3. Radiation source model.

TABLE I
PARAMETERS OF THE RADIATION SOURCE MODEL

EM radiation source	Two half-wavelength dipoles
Position of source	$P_1 = (-0.4\lambda, 0.4\lambda)$ $P_2 = (0.2\lambda, -0.2\lambda)$
Carrier frequency	$f_c = 1$ GHz
Frequency difference	Δf
Input current	$I_0 = 1$ A
Sampling period	$\Delta t = 10$ ns
Sampling number	$K = 100$
Acquisition time	$T = K\Delta t = 1$ μ s
Noise environment	SNR = 10, 20, 30 dB, noise free

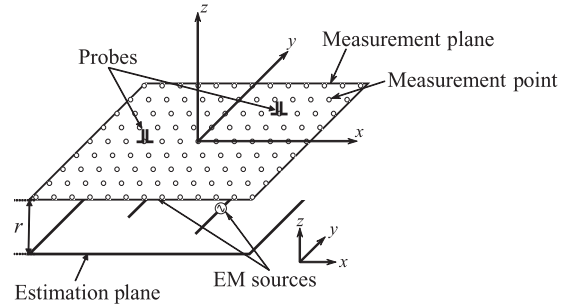


Fig. 4. Simulation model.

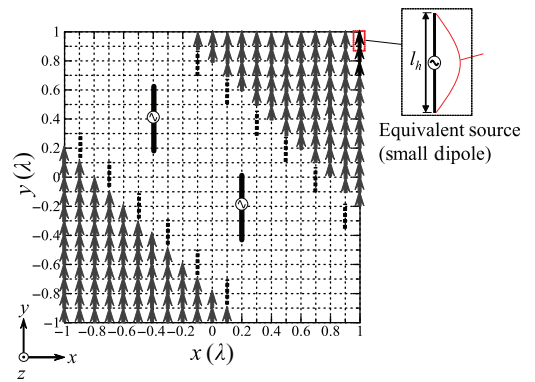


Fig. 5. Model of the equivalent source.

source composed of 0.1λ electrically small dipole antennas is located at equally spaced meshes of 0.1λ space. The total number of the equivalent source M is 420. As the center frequency of the sources is 1 GHz, the mutual impedance matrix \mathbf{Z} is also calculated at 1 GHz.

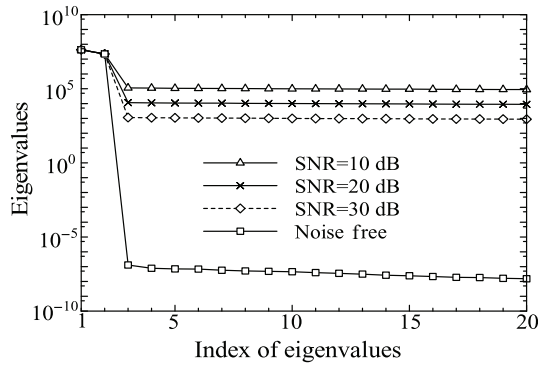


Fig. 6. Eigenvalues ($\Delta f = 500$ kHz).

As a result of applying the eigenvalue decomposition to the correlation matrix \mathbf{C} generated by time-domain measurement, eigenvalues are obtained as shown in Fig. 6, in which only the top 20 eigenvalues are plotted. It is found that the first and the second eigenvalues are significantly larger than others, thus these can be considered as signal components generated by the modulated signals. This means that the near field from the radiation source in Fig. 3 can be expressed equivalently as the coherent near field $\lambda_1\phi_1, \lambda_2\phi_2$ which are orthogonal to each other. From this figure, it can also be said that the eigenvalues of signal components are independent of noise. Furthermore, in this case, it can be observed that the number of eigenvalues of the signal components corresponds to the number of frequency components included in the radiation source.

Let the equivalent near field obtained by the near field measurement be \mathbf{V} vector composed of $\lambda_1\phi_1, \lambda_2\phi_2$. Substituting \mathbf{V} vector and \mathbf{Z} matrix in $\mathbf{V} = \mathbf{Z}\mathbf{I}$, the total current \mathbf{I} vector composed of $\mathbf{I}_1, \mathbf{I}_2$ representing the equivalent current distribution on the equivalent source is obtained. The current distributions indicate where each current mode is distributed. Consequently, it is necessary to add together each current distribution to estimate the position of all radiation sources. The total current \mathbf{I} on the equivalent source is obtained by adding \mathbf{I}_1 and \mathbf{I}_2 together as $|\mathbf{I}| = \sqrt{|\mathbf{I}_1|^2 + |\mathbf{I}_2|^2}$. Numerical simulation for source estimation was carried out by changing three parameters, i.e., the distance r between the estimation plane and the measurement plane, the measurement point N , and the frequency difference Δf . The result of source estimation for each parameter is shown in Figs. 7–9, respectively. This measurement requires a short measurement distance below half a wavelength. This is because we have to construct the equivalent current distribution by inverting the impedance matrix relating the equivalent current elements to the probe. If the distance between the probe and the equivalent current elements is long, the matrix will be more singular and hard to be inverted accurately. The simulation results in Fig. 7 supported this assumption by showing that the estimation accuracy is degraded when the distance r becomes long. Also, the estimation accuracy is increased when the number of measurement points becomes large. Furthermore, it is found that the estimation accuracy becomes worse when the bandwidth of the radiation spectrum increases. These numerical results provide important guidelines to determine the parameters of near field

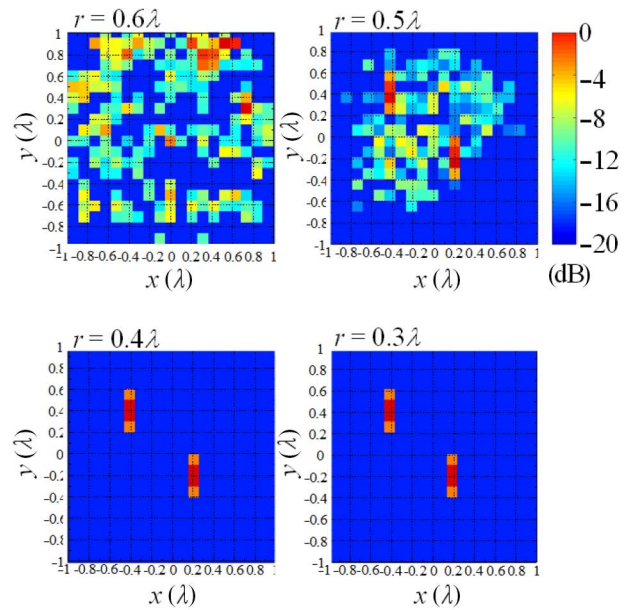


Fig. 7. Current distribution $|\mathbf{I}|$ for different r ($N = 625, M = 420$).

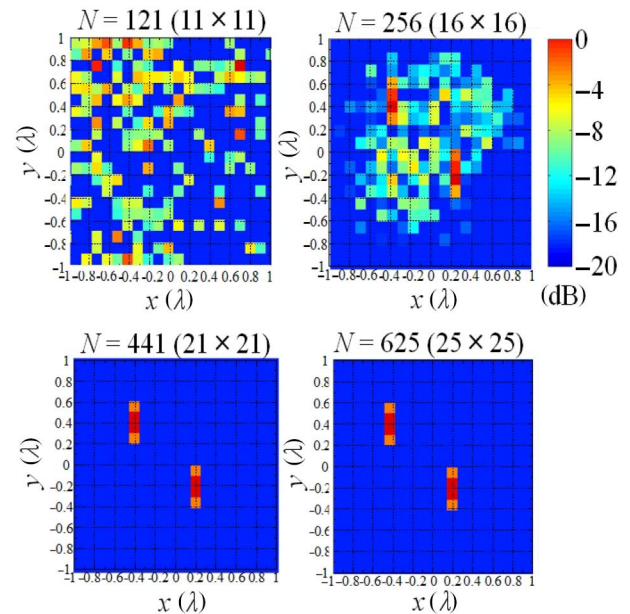


Fig. 8. Current distribution $|\mathbf{I}|$ for different N ($r = 0.3\lambda, M = 420$).

measurement to increase the accuracy and stability of proposed method. A more detailed study on the relation between measurement parameters and accuracy of microwave imaging was carried out in our previous research [3]. These preexamined results will be referred in the experiment in Section IV.

IV. EXPERIMENT

A. Estimation for Dipole Antennas

To demonstrate the validity of the proposed method, the experiment was performed using the same parameters of source model and equivalent source model as in Section III. The near field measurement system is illustrated in Fig. 10. To make the correlation matrix \mathbf{C} , near field was measured simultaneously

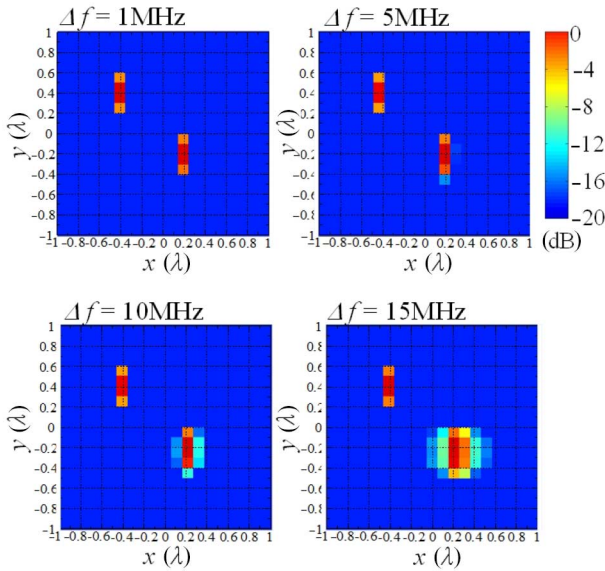


Fig. 9. Current distribution $|I|$ for different Δf ($r = 0.3\lambda$, $M = 625$).

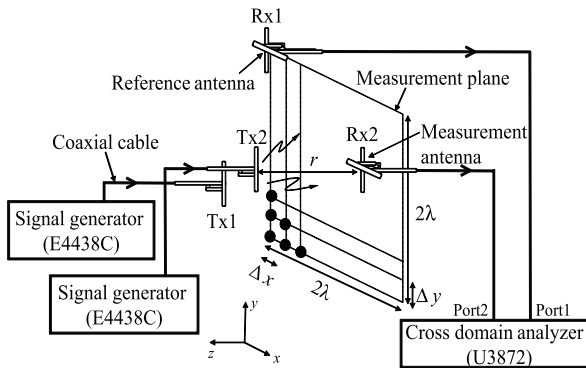


Fig. 10. Experimental system.

at two measurement points by scanning measurement antennas Rx 1 and Rx 2 at the measurement plane. A linear dipole antenna was used as the measurement antenna called scanning probe. The dipole antenna was electrically small and was fed by a coaxial cable with a balun. This consideration for the probe design is to ensure that the probe does not give much influence on the original current distribution of the EM radiation source to increase the accuracy of the near field measurement results because the validity and accuracy of the equivalent current distribution depend largely on the accuracy of the near field measurement results.

It should be noted here that it is a time-consuming measurement to establish the matrix \mathbf{C} containing $2N \times 2N$ elements. Usually, $2N \times 2N$ is a very large number and each matrix element requires measurement data from the simultaneous measurement of the two probes. A two-channel RF receiver for the two probes is also required in the measurement system. In this research, a so-called cross-domain analyzer (Advantest U3872) was used as the receiver which is capable of comparative measurement of the time-domain signals from two channels with a maximum bandwidth of 40 MHz by simultaneous and synchronized measurement.

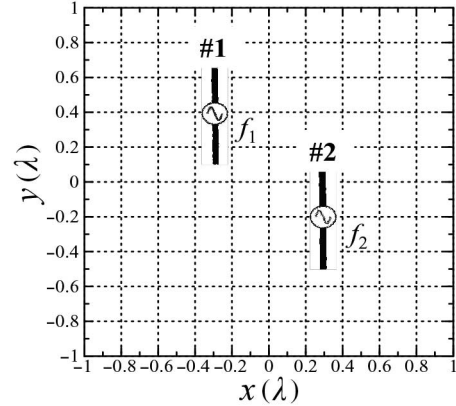


Fig. 11. Radiation source model.

TABLE II
PARAMETERS FOR NEAR FIELD MEASUREMENT

EM radiation source	Two vertical half-wavelength dipoles
Position of source (Model 1)	$P_1 = (-0.4\lambda, 0.4\lambda)$ $P_2 = (0.2\lambda, -0.2\lambda)$
Position of source (Model 2)	$P_1 = (-0.5\lambda, 0.4\lambda)$ $P_2 = (0.3\lambda, -0.3\lambda)$
Carrier frequency	f_1, f_2
Frequency difference	$\Delta f = f_1 - f_2 $
Measurement area	$2\lambda \times 2\lambda$
Total number of measurement points	$N = 625$ (25×25)
Distance from source plane	$r = 0.2\lambda$
Interval of measurement points	$\Delta x = \Delta y = 0.08\lambda$
Number of sampling points	$K = 1001$
Acquisition time	$T = 20$ ms

The radiation sources were two half-wavelength dipole antennas which were vertically mounted in the y -direction, and their relative position is shown in Fig. 11. The distance r between the estimation plane and measurement plane should be small enough to obtain a high signal-to-noise ratio (SNR) to give accurate estimation results. Parameters for the experimental setup are summarized in Table II. The experiment was carried out for two types of radiation source models. In one model (Model 1), two dipole antennas are fed by different signal generators and radiate 1 and 1.0005 GHz continuous wave, respectively. In the other one (Model 2), one antenna is fed with AM modulated signal of center frequency 1 GHz and modulation factor $m_a = 0.5$, the other dipole is fed with the continuous wave of 1.0005 GHz. The total number of measurement points N was 625 and the measurement distance r was 0.2λ , which was decided based on the numerical analysis in Section III.

Applying the eigenvalue decomposition to the correlation matrix \mathbf{C} generated by the near field measurement, eigenvalues were obtained in both source models as shown in Fig. 12. In both cases, the first eigenvalue and second one can be regarded as signal components generated by the modulated radiation source as they were absolutely larger than others, thus, \mathbf{V} vector composed of $\lambda_1\phi_1, \lambda_2\phi_2$ were obtained.

Equivalent source model was same as the one used in the numerical simulation. The total number of the equivalent source M was 420. Parameters of the equivalent source are shown

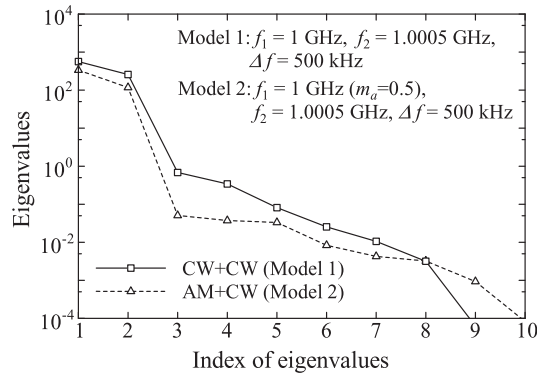


Fig. 12. Eigenvalues.

TABLE III
PARAMETERS OF THE EQUIVALENT SOURCE

Equivalent source	Small dipoles
Frequency for calculation	$f_h = 1$ GHz
Length of equivalent source	$l_h = 0.1 \lambda$
Total number of equivalent source	$M = 420$

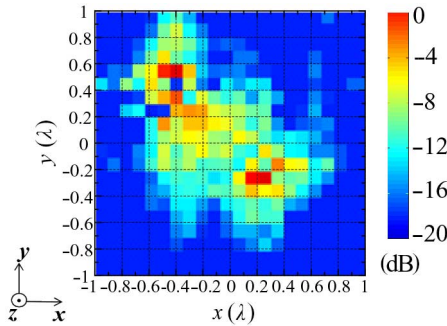


Fig. 13. Equivalent current distribution in Model 1.

in Table III. Numerical calculation of the mutual impedance matrix \mathbf{Z} was performed at 1 GHz.

By solving matrix equation $\mathbf{V} = \mathbf{Z}\mathbf{I}$, \mathbf{I}_1 and \mathbf{I}_2 representing the equivalent current distribution on the equivalent source were obtained. Each result of equivalent current distribution on the equivalent source in both models obtained by near field measurement and the matrix inversion is shown in Figs. 13 and 14, respectively. It was found that the estimated location of sources using the proposed method was coincident with the location of real sources in Fig. 11. Therefore, the validity of the proposed method for modulated radiation signals was demonstrated by experiments.

B. Estimation for Microwave Oven

A microwave oven heats and cooks food by exposing it to electromagnetic radiation at the ISM band approximately 2.45 GHz. Radiation leakage from a microwave oven was measured and the equivalent current of the microwave oven was evaluated using the proposed method. Microwave oven usually has an output spectrum of several MHz of bandwidth. The output power cycle is tied to the 50-Hz ac input cycle; thus, the radiation from the oven is repeated at a periodic time of about 20 ms. Microwave oven using the frequency band of

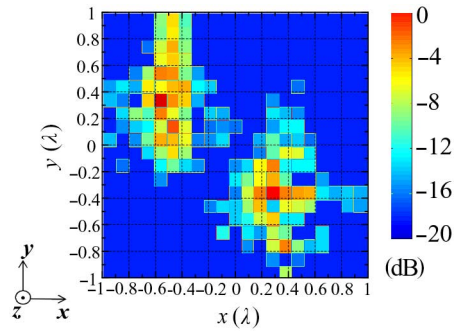


Fig. 14. Equivalent current distribution in Model 2.



Fig. 15. Photograph of experiment in an anechoic chamber.

TABLE IV
PARAMETERS FOR THE EXPERIMENT

EM radiation source	Microwave oven
Center frequency	2.45 GHz
Total number of measurement points	$N = 625 (25 \times 25)$
Distance between the source and measurement plane	$r = 0.2 \lambda$
Number of sampling points	$K = 1001$
Acquisition time	$T = 20$ ms

2.45 GHz is classified into two types such as inverter-type oven and transformer-type oven [14]. As the inverter-type oven has a more complicated structure than that of the transformer-type one, in this measurement, the transformer-type was used as the EM radiation source for estimation. The scene of the measurement in the anechoic chamber is shown in Fig. 15. In the experiment, the microwave oven was driven by 50 Hz ac power and a container full of water was placed in the oven when the oven is in operation. Parameters for the experiment are illustrated in Table IV. The equivalent source model is the same as in the measurement for dipole antennas.

Eigenvalues obtained from the correlation matrix \mathbf{C} generated by the near field measurement are shown in Fig. 16, in which the top 60 eigenvalues are plotted. Because a significant drop in magnitude of these eigenvalues cannot be observed in the figure, it is difficult to distinguish the signal components from the noise components. However, it was known that the estimation result using the top 10 eigenvalues was almost the same as using more eigenvalues. Therefore, the top 10 eigenvalues were used for the following estimation. From Sections III and IV, it was found that the measurement distance r should be less than 0.2λ . Therefore, measurement distance of

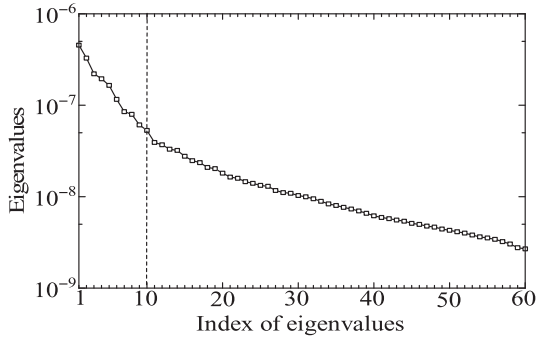


Fig. 16. Eigenvalues.

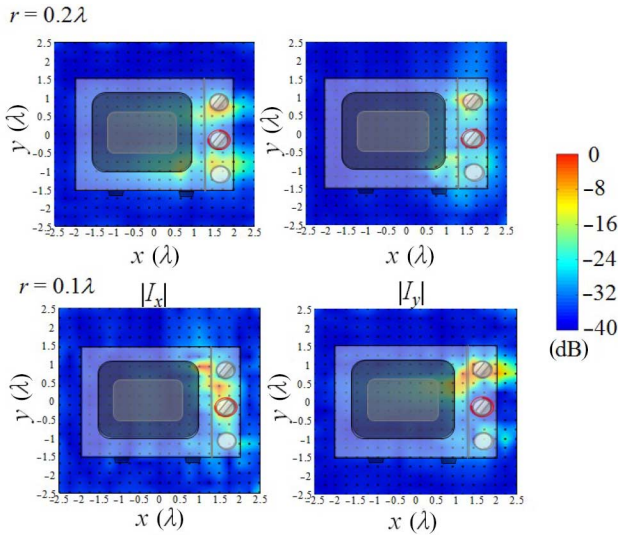


Fig. 17. Estimation results in the front view.

0.1 λ and 0.2 λ was applied to estimate a microwave oven in the experiment. Fig. 17 shows the equivalent current distribution in the estimation plane in front of the oven. From Fig. 17, it can be seen that the estimation result of $r = 0.1\lambda$ is almost same as $r = 0.2\lambda$. In addition, the results of the estimation plane, which was set on the left side, right side, and rear side of the oven when the distance r was 0.1 λ , are also shown in Figs. 18–20, respectively. In these figures, the left one is the horizontally polarized component of the equivalent current and the right one is the vertically polarized component. From these figures, it is found that the equivalent current at the front plane is significantly larger than that on the other measurement planes. Although it is assumed that there are individual differences in characteristics for each microwave oven, it is observed that the estimated distribution of equivalent current mainly occurs in the vicinity of the dial of the microwave oven for this microwave oven.

V. SUMMARY

In this paper, a method to estimate the equivalent current distribution of the modulated radiation source was proposed and the demonstration of the method was conducted using numerical simulations and experiments. In this method, the near field of the source was measured in time domain, and then the eigenvalues and eigenfunctions generated from the correlation

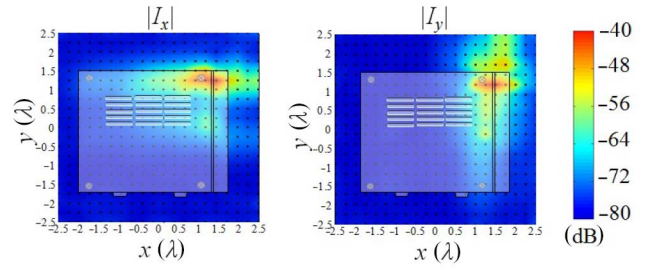


Fig. 18. Estimation results in the left-hand side view.

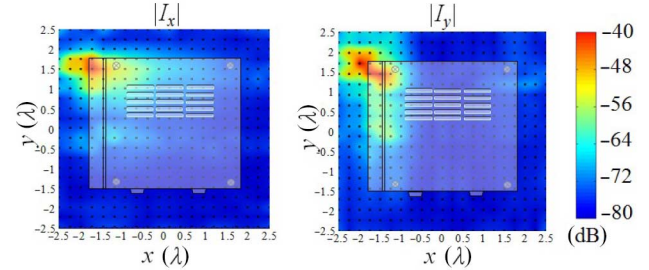


Fig. 19. Estimation results in the right-hand side view.

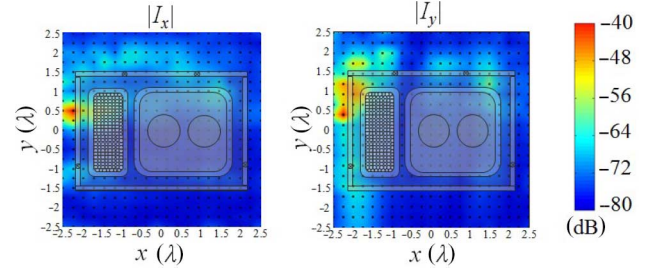


Fig. 20. Estimation results in the rear view.

matrix based on the near field were applied to construct the modulated EM radiation source using the inverse matrix method. In the simulation, estimation was performed on the modulated radiation source composed of dipole antennas, which showed the validity of the proposed method. In the experiment, the equivalent current distribution of two types of source models, which were two dipole antennas and a microwave oven, were estimated. It can be said that the proposed method is effective for the estimation of the equivalent current distribution of the modulated radiation source. Theoretically speaking, this the equivalent current distribution can be transferred to the far field. As demonstrated in the studies of [5], [6], the far field pattern transferred from the near field measurement of the modulated radiation in time domain is equal to the rms value of the far field pattern of the modulated radiation. It is our future work to define and measure the far field pattern for the modulated source in a practical sense which could be helpful to efficiently diagnose EM interference from the modulated EM source.

ACKNOWLEDGMENT

The authors would like to thank Dr. K. Sawaya, Prof. Emeritus of Tohoku University, and Mr. R. Onodera and Mr. T. Sayama, former graduate students of Tohoku University, for their contribution to this paper.

REFERENCES

- [1] P. Petre and T. K. Sarkar, "Near-field to far-field transformation using an equivalent magnetic current approach," *IEEE Trans. Antennas Propag.*, vol. 40, no. 11, pp. 1348–1356, Nov. 1992.
- [2] A. Taaghoul and T. K. Sarkar, "Near-field to near/far-field transformation for arbitrary near field geometry, utilizing an equivalent magnetic current," *IEEE Trans. Electromagn. Compat.*, vol. 38, no. 3, pp. 536–542, Aug. 1996.
- [3] Q. Chen, S. Kato, and K. Sawaya, "Estimation of current distribution on multilayer printed circuit board by near-field measurement," *IEEE Trans. Electromagn. Compat.*, vol. 50, no. 2, pp. 399–405, May 2008.
- [4] S. Kato, Q. Chen, and K. Sawaya, "Current estimation on multi-layer printed circuit board with lumped circuits by near-field measurement," *IEICE Trans. Commun.*, vol. E91B, no. 11, pp. 3788–3791, Nov. 2008.
- [5] B. Fourestie, Z. Altman, J.-C. Bolomey, J. Wiert, and F. Brouay, "Statistical model analysis applied to near-field measurements of random emissions," *IEEE Trans. Antennas Propag.*, vol. 50, no. 12, pp. 1803–1812, Dec. 2002.
- [6] B. Fourestie, J.-C. Bolomey, T. Sarrebourse, Z. Altman, and J. Wiert, "Spherical near field facility for characterizing random emissions," *IEEE Trans. Antennas Propag.*, vol. 53, no. 8, pp. 2582–2589, Aug. 2005.
- [7] B. Nishina, Q. Chen, K. Sawaya, and Q. Yuan, "Construction of equivalent source for modulated electromagnetic radiation," in *Proc. Eur. Conf. Antennas Propag.*, 2014, pp. 156–159.
- [8] G. C. Carter, *Coherence and Time Delay Estimation*. Piscataway, NJ, USA: IEEE Press, 1992.
- [9] F. Smithies, *Integral Equations*. Cambridge, U.K.: Cambridge Univ. Press, 1970, p. 128.
- [10] E. Wolf, "New theory of partial coherence in the space-frequency domain. Part I: Spectra and cross spectra of steady-state sources," *J. Opt. Soc. Amer.*, vol. 72, pp. 343–351, Mar. 1982.
- [11] R. F. Harrington, *Field Computation by Moment Methods*. Hoboken, NJ, USA: Wiley, 1993.
- [12] J. H. Richmond and N. H. Geary, "Mutual impedance of nonplanar-skew sinusoidal dipoles," *IEEE Trans. Antennas Propag.*, vol. 23, no. 3, pp. 412–414, May 1975.
- [13] C. W. Chuang, J. H. Richmond, N. Wang, and P. H. Pathak, "New expressions for mutual impedance of nonplanar-skew sinusoidal monopoles," *IEEE Trans. Antennas Propag.*, vol. 38, no. 2, pp. 275–276, Feb. 1990.
- [14] Y. Yamanaka and T. Shinozuka, "Statistical parameter measurement of unwanted emission from microwave ovens [digital mobile radio interference]," in *Proc. IEEE Int. Symp. Electromagn. Compatibil.*, 1995, pp. 57–61.



Bunka Nishina graduated from Faculty of Engineering, Tohoku University, Sendai, Japan in 2013, and received the M.E. degree in the subject of Communications Engineering from Graduate School, Tohoku University in 2015.

During his M.E. study, he did research on the electromagnetic inverse problem. He joined KDDI Corporation, Tokyo, Japan in 2015.



Qiang Chen (M'94–SM'12) received the B.E. degree in the subject of Electromagnetic Engineering from Xidian University, Xi'an, China, in 1986, the M.E. and D.E. degrees in the subject of Electrical and Communication Engineering from Graduate School, from Tohoku University, Sendai, Japan, in 1991 and 1994, respectively.

He is currently a Chair Professor of Electromagnetic Engineering Laboratory, Department of Communications Engineering, School of Engineering, Tohoku University. His

research interests include antennas, microwave and millimeter wave, electromagnetic measurement, and computational electromagnetics.

Dr. Chen is a member of the IEICE. He was the Secretary and Treasurer of IEEE Antennas and Propagation Society Tokyo Chapter in 1998, the Secretary of Technical Committee on Electromagnetic Compatibility of IEICE from 2004 to 2006, the Secretary of Technical Committee on Antennas and Propagation of IEICE from 2008 to 2010, Associate Editor of *IEICE Transactions on Communications* from 2007 to 2012. He served as a Chair of IEICE Technical Committee on Photonics-Applied Electromagnetic Measurement from 2012 to 2014. He was the recipient of the Young Scientists Award in 1993, the Best Paper Award and Zen-ichi Kiyasu Award in 2009 from the Institute of Electronics, Information and Communication Engineers (IEICE) of Japan.